Associated charged Higgs and W boson production in the MSSM at the LHC

David Eriksson[1], Stefan Hesselbach[2a], and Johan Rathsman[1]

[1] High Energy Physics, Uppsala University, Box 535, S-75121 Uppsala, Sweden
[2] School of Physics & Astronomy, University of Southampton, Highfield, Southampton SO17 1BJ, UK

Abstract. We investigate the associated production of charged Higgs bosons ($H^\pm$) and W bosons at the CERN Large Hadron Collider, using the leptonic decay $H^+ \to \tau^+\nu_\tau$ and hadronic W decay, within different scenarios of the Minimal Supersymmetric Standard Model (MSSM) with both real and complex parameters. Performing a parton level study we show how the irreducible Standard Model background from $W+2$ jets can be controlled by applying appropriate cuts. In the standard $m_h^{\rm max}$ scenario we find a viable signal for large $\tan\beta$ and intermediate $H^\pm$ masses ($\sim m_t$). In MSSM scenarios with large mass-splittings among the heavy Higgs bosons the cross-section can be resonantly enhanced by factors up to one hundred, with a strong dependence on the CP-violating phases.

PACS. 14.80.Cp Non-standard-model Higgs bosons – 12.60.Jv Supersymmetric models

1 Introduction

One of the main tasks at the upcoming experiments at the CERN Large Hadron Collider (LHC) is the determination of the mechanisms of electroweak symmetry breaking and of the generation of elementary particle masses. In the Minimal Supersymmetric Standard Model (MSSM), which is a two Higgs Doublet Model (2HDM) of type II, the Higgs sector consists of three neutral and one charged Higgs bosons after electroweak symmetry breaking. The charged Higgs boson ($H^\pm$) is of special interest since its discovery would constitute an indisputable proof of physics beyond the Standard Model (SM).

The main production mode of charged Higgs bosons at hadron colliders is in association with top quarks through the $gb \to H^- t$ and $gg \to H^- t\bar{b}$ processes [1,2,3,4,5,6,7] with the former one being dominant for heavy charged Higgs bosons $m_{H^\pm} \gtrsim m_t$ and the latter one for light ones $m_{H^\pm} \lesssim m_t - m_b$. A complementary production mode of charged Higgs bosons is in association with W-bosons [8,9,10,11,12,13,14]. Although the production cross-section [8,9] is large, an earlier study [10] using the hadronic charged Higgs decay, $H^+ \to t\bar{b}$, came to the conclusion that the signal is overwhelmed by the $t\bar{t}$ background.

Here, we report results of our study [13] of the prospects of using instead the $H^+ \to \tau^+\nu_\tau$ decay together with $W \to 2$ jets in the MSSM with both real and complex parameters. In the following we first outline the simulation of $H^\pm W^\mp$ production and decay at the LHC and then give our results for the standard maximal mixing ($m_h^{\rm max}$) scenario as well as for scenarios with resonantly enhanced cross section. For more details we refer to [13].

2 Simulation and signal selection

The dominant production mechanisms for $H^\pm W^\mp$ at hadron colliders are $b\bar{b}$ annihilation at tree-level and gluon fusion at one-loop-level. Here, we focus on the parameter region with intermediate $H^\pm$ masses ($\sim m_t$) and large $\tan\beta$, where the decay $H^\pm \to \tau\nu_\tau$ has a large branching ratio and where the $b\bar{b}$ annihilation dominates. We have implemented [15] the two processes $b\bar{b} \to H^+W^-$ and $b\bar{b} \to H^-W^+$ as separate external processes to PYTHIA [16]. For the calculation of the MSSM scenario and the corresponding Higgs masses and the branching ratios of $H^\pm$ we use FEYNHIGGS 2.2.10 [17]. We only consider hadronic τ decays, $\tau \to \nu_\tau + \tau_{\rm jet}$, which are performed using the program TAUOLA [18] in order to properly take into account the spin effects, resulting in the signature $2j + \tau_{\rm jet} + \not{p}_\perp$. The dominant irreducible SM background arises from W + 2 jets production which we have simulated with help of the package ALPGEN [19] again complemented with TAUOLA to perform the τ decay.

Since this study is performed at parton level, without any parton showering or hadronisation, the momenta of the jets are smeared as a first approximation to take these, as well as detector effects, into account. After smearing the following basic cuts are applied: $|\eta_{\tau_{\rm jet}}| < 2.5$, $|\eta_j| < 2.5$, $\Delta R_{jj} > 0.4$, $\Delta R_{\tau_{\rm jet} j} > 0.5$, and $p_{\perp{\rm jet}} > 20$ GeV. We then apply the further cuts given in table 1 in order to suppress the background,

[a] *Email:* s.hesselbach@phys.soton.ac.uk

Table 1. The effect of the different cuts on the integrated cross-section for background ($\sigma_{\rm b}$) and signal ($\sigma_{\rm s}$) in the $m_h^{\rm max}$ scenario with $m_{H^\pm} = 175$ and 400 GeV for $\tan\beta = 50$ as well as the number of signal events S and the significance $S/\sqrt{B}$ assuming an integrated luminosity of 300 fb^{-1} and a τ detection efficiency of 30% .

		$m_{H^\pm} = 175$ GeV			$m_{H^\pm} = 400$ GeV		
Cut [all in GeV]	$\sigma_{\rm b}$ (fb)	$\sigma_{\rm s}$ (fb)	S	$S/\sqrt{B}$	$\sigma_{\rm s}$ (fb)	S	$S/\sqrt{B}$
Basic cuts	560000	55	4900	0.7	3.3	300	0.04
$p_{\perp\tau_{\rm jet}} > 50$, $\not{p}_\perp > 50$	22000	25	2200	1.6	2.7	240	0.2
$70 < m_{jj} < 90$	1700	21	1900	5	2.2	200	0.5
$m_\perp > 100$	77	15	1400	16	2.1	190	2.3
$p_{\perp hj} > 50$, $p_{\perp sj} > 25$	28	9.3	840	17	1.5	135	2.6

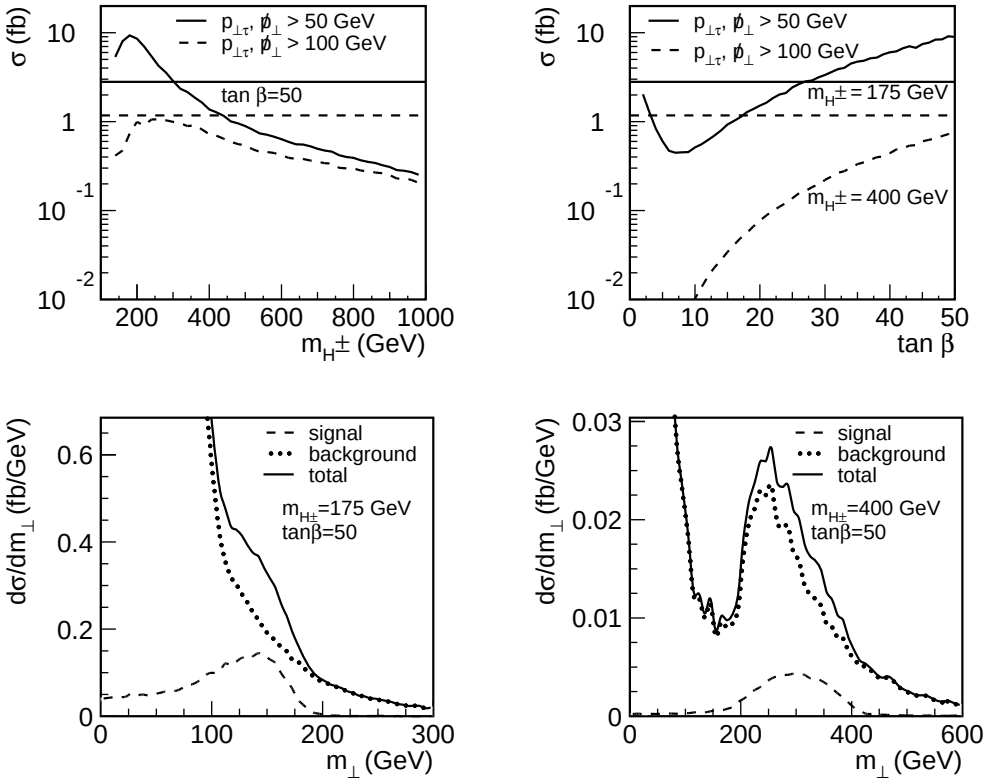

Fig. 1. Upper row: $H^\pm$ mass and $\tan\beta$ dependence of the integrated cross-section in the $m_h^{\rm max}$ scenario. Solid curves are with all cuts of table 1 and dashed curves are with the harder cuts $p_{\perp\tau_{\rm jet}}, \not{p}_\perp > 100$ GeV. The horizontal lines correspond to $S/\sqrt{B} = 5$. Lower row: $m_\perp$ distribution for the signal (dashed) in the $m_h^{\rm max}$ scenario with $\tan\beta = 50$ and $m_{H^\pm} = 175$ GeV (left) as well as $m_{H^\pm} = 400$ GeV (right) together with the background (dotted) with all cuts of table 1 (for $m_{H^\pm} = 400$ GeV the cuts $p_{\perp\tau_{\rm jet}}, \not{p}_\perp > 100$ GeV are used).

where $m_\perp = \sqrt{2p_{\perp\tau_{\rm jet}}\not{p}_\perp[1-\cos(\Delta\phi)]}$ (with $\Delta\phi$ being the azimuthal angle between $p_{\perp\tau_{\rm jet}}$ and $\not{p}_\perp$) is the transverse mass and $p_{\perp hj}$ ($p_{\perp sj}$) is the harder (softer) of the two jets. The cuts $\not{p}_\perp, p_{\perp\tau_{\rm jet}} > 50$ GeV are primarily included to take the reducible QCD background into account, which has not been simulated explicitly. In order to estimate the sensitivity of the final results due to this choice we have also used an alternative set of harder cuts, $\not{p}_\perp, p_{\perp\tau_{\rm jet}} > 100$ GeV.

3 Standard MSSM scenarios

The signal cross-sections in the standard $m_h^{\rm max}$ scenario as well as the resulting number of events and the significance $S/\sqrt{B}$ are given in table 1 for the MSSM parameters $\mu = 200$ GeV, $M_{\rm SUSY} = 1$ TeV, $A_t = A_b = A_\tau = 2$ TeV, $M_2 = 200$ GeV, and $m_{\tilde{g}} = 800$ GeV. The upper row in fig. 1 shows the $m_{H^\pm}$ and $\tan\beta$ dependence of the cross-section after all cuts of table 1 (solid curves) and after the harder cuts $p_{\perp\tau_{\rm jet}}, \not{p}_\perp > 100$ GeV (dashed curves). The horizontal lines indicate the cross-section needed for $S/\sqrt{B} = 5$, corresponding to $\tan\beta \gtrsim 30$ if $m_{H^\pm} = 175$ GeV and 150 GeV $\lesssim m_{H^\pm} \lesssim$ 300 GeV if $\tan\beta = 50$ with the softer cuts $p_{\perp\tau_{\rm jet}}, \not{p}_\perp > 50$ GeV, whereas with the harder cuts $\tan\beta$ has to be larger than at least 50.

The lower row in fig. 1 shows the resulting $m_\perp$ distribution for $m_{H^\pm} = 175$ GeV as well as $m_{H^\pm} = 400$ GeV in the case $\tan\beta = 50$ compared to the background after all cuts in table 1 have been applied.

Table 2. MSSM parameters for the resonant scenario in addition to $M_L^3 = M_E^3 = 500$ GeV, $A_t = A_b = 0$, $M_2 = m_{\tilde{g}} = 500$ GeV as well as the range for the scan of parameters together with the step size.

	MSSM parameters. All masses in GeV.					
	$m_{H^\pm}$	$\tan\beta$	μ	M_Q^3	M_U^3	M_D^3
Res. scen.	175	11	3300	250	250	400
Scan min	100	1	1800	150	150	150
Scan max	450	40	3300	650	650	650
Step size	25	1	250	50	50	50

In the high mass case the harder cuts $p_{\perp\tau_{\rm jet}}, \not{p}_\perp > 100$ GeV are used giving $S/\sqrt{B} = 3.2$. Applying an upper cut $m_\perp < 200$ GeV ($m_\perp < 500$ GeV) for $m_{H^\pm} = 175$ GeV ($m_{H^\pm} = 400$ GeV) only marginally improves $S/\sqrt{B}$ from 17 (3.2) to 19 (3.3). In the same figure we also see that the harder cuts create a fake peak in the background. Finally, using the harder cuts $p_{\perp\tau_{\rm jet}}, \not{p}_\perp > 100$ GeV the significance for $m_{H^\pm} = 175$ GeV and $\tan\beta = 50$ is reduced to $S/\sqrt{B} = 3.1$. However, in this case using an upper cut $m_\perp < 200$ GeV is beneficial leading to a significance of $S/\sqrt{B} = 6.4$.

The above results in standard MSSM scenarios depend only weakly on the underlying MSSM parameter point except for parameter points with large mass splitting between charged and neutral Higgs bosons which will be described in the next section.

4 Resonant scenarios

In MSSM parameter regions with $|\mu|, |A_t|$, or $|A_b| > 4M_{\rm SUSY}$ the dominant terms of the 1-loop corrections to the quartic couplings in the Higgs sector [20] can induce a large mass splitting between the charged and neutral Higgs bosons [21,22]. A scan over the relevant parameters shows that scenarios with $m_A > m_{H^\pm} + m_W$ are possible in a large range in both $\tan\beta$ and $m_{H^\pm}$ [13]. On average 0.2% of the scanned MSSM scenarios as outlined in table 2 turn out to fulfil this relation. In this case the cross section for $b\bar{b} \to H^\pm W^\mp$ can be considerably enhanced through the resonance of a Higgs boson in the s-channel.

Figure 2 shows the resulting $m_\perp$-distribution compared to the background in the resonant scenario of table 2. In case of resonant production, the $H^\pm$ and W bosons are produced with typically small transverse momenta. Thus it is favourable to loosen the cuts on the light jets from the W. Applying the basic and additional cuts from table 1, except the cuts $p_{\perp hj} > 50$ GeV and $p_{\perp sj} > 25$ GeV on the light jets, we get an integrated cross-section of 52 fb for a charged Higgs boson mass of 175 GeV corresponding to a significance $S/\sqrt{B} = 56$. For comparison, if we apply the harder cuts $p_{\perp\tau_{\rm jet}} > 100$ GeV and $\not{p}_\perp > 100$ GeV in this resonant case the significance is reduced drastically to $S/\sqrt{B} = 0.2$ due to the typically small transverse momentum of the $H^\pm$-boson. Thus, in the case of harder cuts the resonantly enhanced cross-section is only of use if $m_{H^\pm}$ is large enough such that $m_{H^\pm}/2$ is well above 100 GeV.

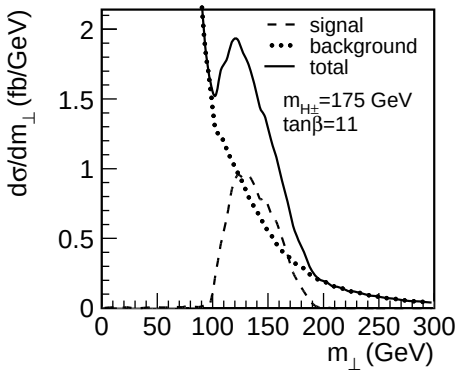

Fig. 2. The $m_\perp$ distribution of the signal (dashed) in the resonant scenario of table 2 and of the background (dotted) with all cuts of table 1 except $p_{\perp hj} > 50$ GeV and $p_{\perp sj} > 25$ GeV.

The study of these resonant scenarios also illustrates what could happen in a general 2HDM, where the Higgs boson masses are more or less independent parameters and the resonant scenarios are less fine-tuned.

5 MSSM with complex parameters

In the general MSSM many parameters can be complex. Then explicit CP violation occurs also in the Higgs sector through loops of supersymmetric particles [20,23], which affects our signal process because of the neutral Higgs bosons exchanged in the s-channel. The leading contributions to CP violation in the neutral Higgs sector arise from loops of the scalar top and (to a lesser extend) of the scalar bottom sector where the possibly complex Higgs/higgsino mass parameter μ and the trilinear scalar couplings A_t and A_b are dominant. Hence, assuming $\phi_{A_b} = \phi_{A_t}$ we concentrate in the following on the phases ϕ_μ and ϕ_{A_t} of μ and A_t, respectively, which have the largest effect on the neutral Higgs sector and thus possibly affect our signal. Despite the fact that the SUSY phases may be severely constrained by bounds on the Electric Dipole Moments (EDMs), these constraints are rather model dependent and may be evaded in scenarios with heavy first and second generation sfermions, due to cancellations among various contributions to the EDMs or due to additional contributions from lepton flavour violating terms in the Lagrangian, for a review see e.g. [24]. Thus, we have varied ϕ_μ and ϕ_{A_t} independently in the range $-\pi < \phi < \pi$ in order to investigate the phase dependence of our signal.

In standard MSSM scenarios, such as the $m_h^{\rm max}$ scenario, we find only small ($\sim 5\%$) ϕ_μ and ϕ_{A_t} dependencies of our signal cross-section as shown in the left plot in fig. 3. The right plot in fig. 3 shows the dependence of the cross-section on ϕ_μ in the resonant scenario of table 2, where the Higgs masses, couplings and widths have been calculated with FeynHiggs at one-loop ac-

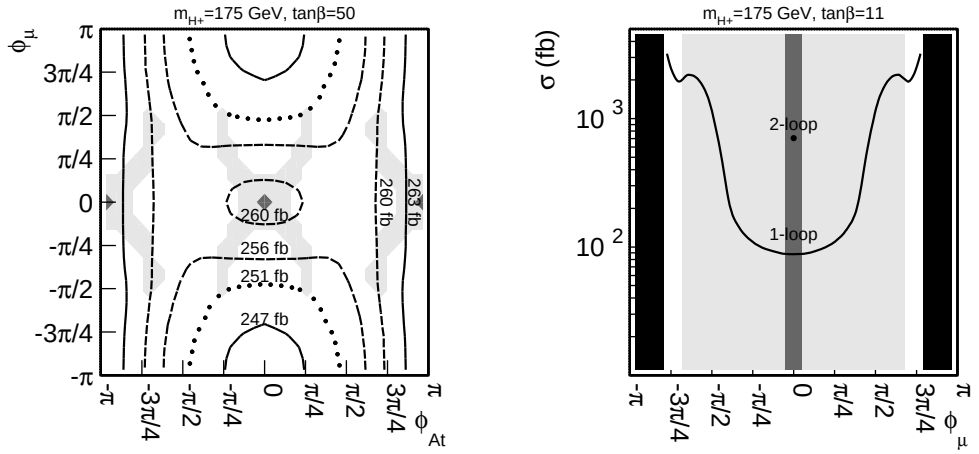

Fig. 3. Left plot: Contours of the total cross-section in the $m_h^{\max}$ scenario. Right plot: Total cross-section in the resonant scenario of table 2 with the Higgs masses etc. calculated to one-loop. For comparison the result with all available corrections for $\phi_\mu = 0$ is also shown. The light shaded areas are in agreement with the constraints from a_μ and $\delta\rho_0$ and the dark shaded ones are also in agreement with the constraints from EDMs. In the black areas numerical instabilities occurred in the calculation of the Higgs masses and mixing matrix.

curacy[1]. The very large phase dependence in this scenario is due to the fact that the production goes from non-resonant to resonant when the phase is varied. More specifically, we get $m_A = m_{H_3} = 246$ GeV for $\phi_\mu = 0$ in the 1-loop case, which is below the resonant threshold, whereas $m_{H_3} = 342$ GeV for the largest values of ϕ_μ where we got a stable result, which is clearly in the resonant regime.

In principle, the process under study also offers the possibility to explore effects of CP violation via a CP-odd rate asymmetry $A_{\rm CP}$ between $\sigma(pp \to H^+W^-)$ and $\sigma(pp \to H^-W^+)$. However, in all considered MSSM scenarios we find that $A_{\rm CP}$ is smaller than about 1%.

This work has been supported by the Göran Gustafsson Foundation.

References

1. R. M. Barnett, H. E. Haber, and D. E. Soper, Nucl. Phys. **B306** (1988) 697.
2. A. C. Bawa, C. S. Kim, and A. D. Martin, Z. Phys. **C47** (1990) 75.
3. F. Borzumati, J.-L. Kneur, and N. Polonsky, Phys. Rev. **D60** (1999) 115011, hep-ph/9905443.
4. D. J. Miller, S. Moretti, D. P. Roy, and W. J. Stirling, Phys. Rev. **D61**, (2000) 055011, hep-ph/9906230.
5. J. Alwall and J. Rathsman, JHEP **0412** (2004) 050, hep-ph/0409094.
6. B. Mohn, M. Flechl, and J. Alwall, ATLAS discovery potential for the Charged Higgs Boson in $H^+ \to \tau\nu$ decays, ATL-PHYS-PUB-2007-006, 2007.
7. S. Hesselbach, S. Moretti, J. Rathsman and A. Sopczak, arXiv:0708.4394 [hep-ph].
8. D. A. Dicus, J. L. Hewett, C. Kao, and T. G. Rizzo, Phys. Rev. **D40** (1989) 787.
9. A. A. Barrientos Bendezu and B. A. Kniehl, Phys. Rev. **D59** (1999) 015009, hep-ph/9807480.
10. S. Moretti and K. Odagiri, Phys. Rev. **D59** (1999) 055008, hep-ph/9809244.
11. O. Brein, W. Hollik, and S. Kanemura, Phys. Rev. **D63** (2001) 095001, hep-ph/0008308.
12. E. Asakawa, O. Brein, and S. Kanemura, Phys. Rev. **D72** (2005) 055017, hep-ph/0506249.
13. D. Eriksson, S. Hesselbach and J. Rathsman, accepted by Eur. Phys. J. **C**, hep-ph/0612198.
14. J. Gao, C. S. Li and Z. Li, arXiv:0710.0826 [hep-ph].
15. D. Eriksson, The fortran code for the $b\bar{b} \to H^+W^-$ and $b\bar{b} \to H^-W^+$ processes are available from `http://www.isv.uu.se/thep/MC/pybbwh/`, including a manual.
16. T. Sjöstrand *et al.*, Comput. Phys. Commun. **135** (2001) 238, hep-ph/0010017.
17. T. Hahn, W. Hollik, S. Heinemeyer, and G. Weiglein, hep-ph/0507009.
18. P. Golonka *et al.*, hep-ph/0312240.
19. M. L. Mangano, M. Moretti, F. Piccinini, R. Pittau, and A. D. Polosa, JHEP **0307** (2003) 001, hep-ph/0206293.
20. A. Pilaftsis and C. E. M. Wagner, Nucl. Phys. **B553** (1999) 3, hep-ph/9902371.
21. A. G. Akeroyd and S. Baek, Phys. Lett. **B525** (2002) 315, hep-ph/0105228.
22. B. Mohn, N. Gollub, and K. A. Assamagan, Study of the $H^\pm \to W^\pm H^0$ decay in a large mass splitting MSSM scenario with ATLAS, ATL-PHYS-PUB-2005-017.
23. A. Pilaftsis, Phys. Lett. **B435** (1998) 88, hep-ph/9805373.
24. K. A. Olive, M. Pospelov, A. Ritz and Y. Santoso, Phys. Rev. **D72** (2005) 075001, hep-ph/0506106.

[1] A calculation with all available corrections is not possible here because the phases lead to numerical instabilities.